

Vanadium oxide metal-insulator phase transition in different types of one-dimensional photonic microcavities

Francesco Scotognella

Dipartimento di Fisica, Politecnico di Milano, piazza Leonardo da Vinci 32, 20133 Milano, Italy

Email: francesco.scotognella@polimi.it

Abstract

The optical properties of vanadium dioxide (VO_2) can be tuned via metal-insulator transition. In this work different types of one-dimensional photonic structure-based microcavities that embed vanadium dioxide have been studied in the spectral range between 900 nm and 2000 nm. In particular, VO_2 has been sandwiched between: i) two photonic crystals made of SiO_2 and ZrO_2 ; ii) two aperiodic structures made of SiO_2 and ZrO_2 that follow the Thue-Morse sequence; iii) two disordered photonic structures, made of SiO_2 and ZrO_2 in which the disorder is introduced either by a random sequence of the two materials or by a random variation of the thicknesses of the layers; iv) two four material-based photonic crystals made of SiO_2 , Al_2O_3 , Y_2O_3 , and ZrO_2 . The ordered structures i and iv show, respectively, one and two intense transmission valleys with defect modes, while the aperiodic and disordered structures ii and iii show a manifold of transmission valleys due to their complex layered configurations. The metal-insulator transition of VO_2 , controlled by temperature, results in a modulation of the optical properties of the microcavities.

Keywords: Photonic crystals; vanadium dioxide; metal-insulator transition.

Introduction

Crystalline vanadium dioxide (VO_2) shows a thermochromic phase transition around 68 °C (341 K) [1]. The phase transition is related to a structural crystal change from a monoclinic insulating phase to a tetragonal (rutile) metallic phase [2,3]. From an optical point of view, the phase transition of VO_2 results in a change from an insulating semi-transparent material from a metallic more lossy and reflective material [3,4]. VO_2 phase transition can be exploited for several applications, such as smart windows, steep-slope devices for micro-electronics, neuromorphic computing devices, and reconfigurable radiofrequency switches [5,6].

A method to utilize VO_2 switchable optical properties is the integration of such material in its integration in photonic crystals [7–9]. In photonic crystals, the periodic modulation of the refractive index in one, two or three dimensions gives rise to energy regions in which light is not transmitted through the crystal. The integration of materials with switchable optical properties in the infrared, such photochromic polymers [10] and infrared plasmonic nanomaterials [11,12], in one-dimensional photonic crystals has been proposed [13].

In this work, we propose different types of one-dimensional photonic microcavities [14], in which a layer of VO_2 is embedded between two photonic crystals, two aperiodic Thue-Morse photonic structures, two disordered photonic structures, and two four-material based photonic crystals. The wavelength dependent refractive indexes of all the employed materials have been used. The light transmission of the microcavities has been simulated via the transfer matrix method. The modulation of the transmission spectra of the microcavities due the VO_2 metal-insulator phase transition has been highlighted.

Methods

The light transmission of the different microcavities in the spectral range between 900 nm and 2000 nm has been studied with the transfer matrix method [15–17]. The system is glass/multilayer/air

with light impinging the sample surface orthogonally. The characteristic matrix of the multilayer is written as

$$M = \begin{bmatrix} M_{11} & M_{12} \\ M_{21} & M_{22} \end{bmatrix} = \prod_{j=1}^N \begin{bmatrix} \cos\left(\frac{2\pi}{\lambda} n_k(\lambda) d_k\right) & -\frac{i}{n_k(\lambda)} \sin\left(\frac{2\pi}{\lambda} n_k(\lambda) d_k\right) \\ -i n_k(\lambda) \sin\left(\frac{2\pi}{\lambda} n_k(\lambda) d_k\right) & \cos\left(\frac{2\pi}{\lambda} n_k(\lambda) d_k\right) \end{bmatrix} \quad (1)$$

With $k=(1,\dots,N)$ and N number of layers. d_k and $n_k(\lambda)$ are the thickness and the wavelength dependent refractive index of the k th layer, respectively. The light transmission is written as

$$T = \frac{n_0}{n_g} \left| \frac{2n_g}{(M_{11}+M_{12}n_0)n_g+(M_{21}+M_{22}n_0)} \right|^2 \quad (2)$$

With n_g the refractive index of glass and n_0 the refractive index of air ($n_g = 1.46$; $n_0 \cong 1$). The light transmission has been calculated in the selected spectral range with steps of 0.25 nm. The wavelength dependent refractive index $n_k(\lambda)$ can be written with the Sellmeier equation

$$n_k^2(\lambda) - 1 = \sum_{j'=1} \frac{A_{j'} \lambda^2}{\lambda^2 - B_{j'}} \quad (3)$$

The parameters $A_{j'}$ and $B_{j'}$ are reported in Table 1.

Material	A_1	B_1	A_2	B_2	A_3	B_3	Ref.
SiO ₂	0.6961663	0.0684043	0.4079426	0.1162414	0.8974794	9.896161	[18,19]
Al ₂ O ₃	1.023798	0.0614482	1.058264	0.1106997	5.280792	17.92656	[20]
Y ₂ O ₃	2.578	0.1387	3.935	22.936	-	-	[21]
ZrO ₂	1.347091	0.062543	2.117788	0.166739	9.452943	24.32057	[22]

Table 1. Parameters of the Sellmeier equation for SiO₂, Al₂O₃, Y₂O₃, and ZrO₂.

The wavelength dependent refractive indexes of vanadium dioxide in the metal phase and in the insulating phase (30 °C) and in the metallic phase (100 °C) have been taken from Ref. [2].

Results and Discussion

In Figure 1 the light transmission spectrum for the microcavity (SiO₂/ZrO₂)₅/VO₂/(ZrO₂/SiO₂)₅ is shown. The black solid curve is related to VO₂ in the insulating phase, while the blue dashed curve is related to VO₂ in the metallic phase. The two phases correspond to a temperature of the material of 30 °C for the insulating phase and a temperature of 100 °C for the metallic phase, respectively, as reported in Ref. [2]. In the microcavity the thickness of the silicon dioxide layers is 220 nm, the thickness of the zirconium dioxide layers is 165 nm, while the thickness of the vanadium dioxide layers is 55 nm.

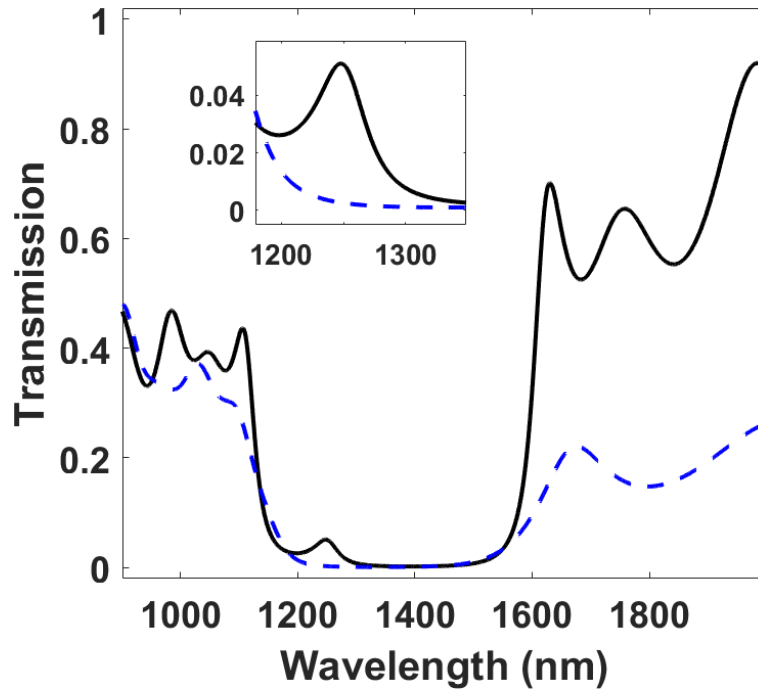


Figure 1. Light transmission spectra for the microcavity $(\text{SiO}_2/\text{ZrO}_2)_5/\text{VO}_2/(\text{ZrO}_2/\text{SiO}_2)_5$ with VO_2 in the insulating phase (at 30 °C, black solid curve) and in the metallic phase (at 100 °C, blue dashed curve).

In the microcavity configuration, the insulating VO_2 based microcavity shows a defect mode at around 1250 nm within the photonic band gap of the structure (i.e. the intense transmission valley between 1100 nm and 1600 nm). The defect mode is magnified in the inset of Figure 1. Instead, for the metallic VO_2 based microcavity the defect mode is suppressed. Noteworthy, the transmission at wavelengths longer than 1600 nm is weaker in the metallic VO_2 because of its infrared absorption.

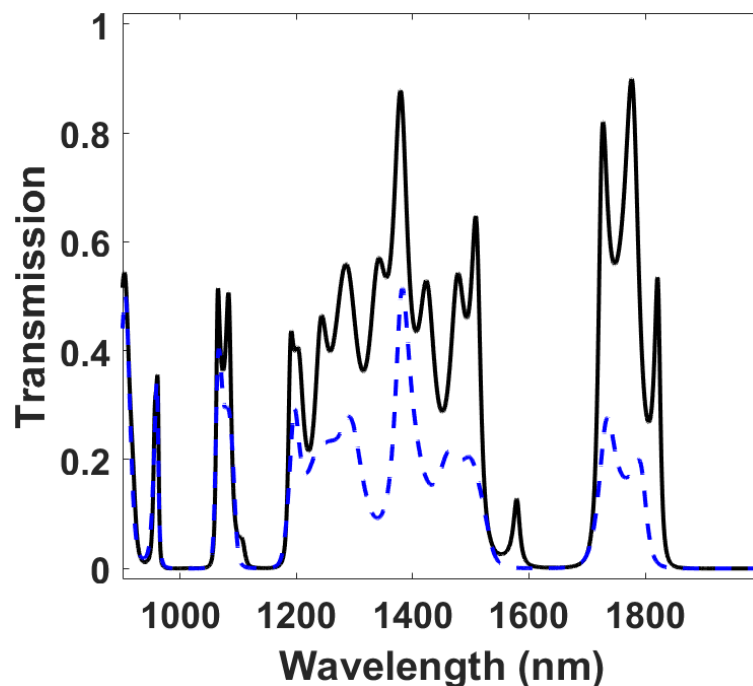


Figure 2. Light transmission spectra for the Thue-Morse aperiodic microcavity $\text{ABBABAABBAABABBABAABABBAABBABAAB}/\text{VO}_2/\text{ABBABAABBAABABBABAABABBAAB}$

BABAAB (A = SiO₂; B = ZrO₂) with VO₂ in the insulating phase (at 30 °C, black solid curve) and in the metallic phase (at 100 °C, blue dashed curve).

In Figure 2 the transmission spectrum for the aperiodic microcavity that follows the Thue-Morse sequence is depicted. VO₂ is sandwiched between two photonic structures with the sequence of layers ABBABAABBAABBABAABABBABAAB [23] (A = SiO₂; B = ZrO₂). The layer thicknesses are the same of the ones of the periodic structure. The black solid curve is related to VO₂ in the insulating phase, while the blue dashed curve is related to VO₂ in the metallic phase. The transmission spectra are slightly modified with the VO₂ from the insulating to the metallic phase, with the suppression of peaks around 1100 and 1600 nm.

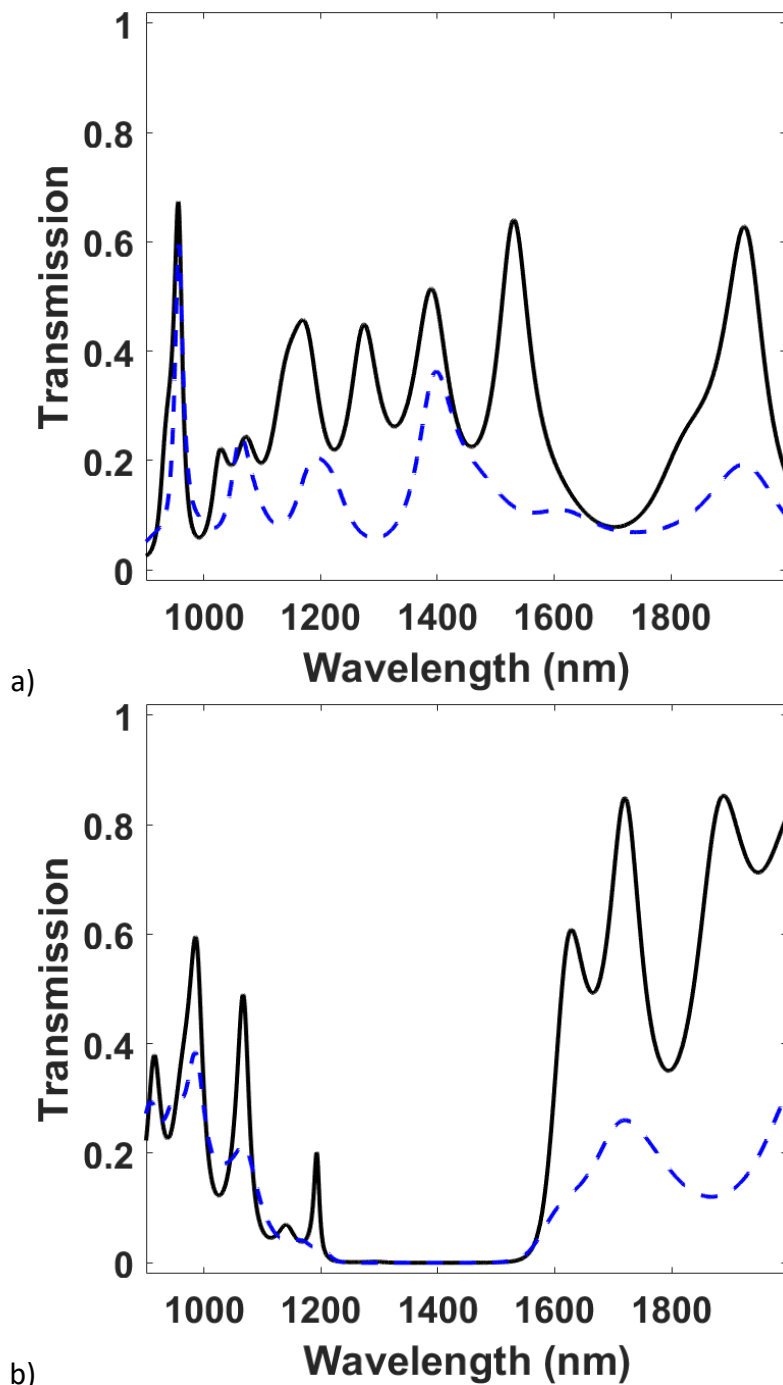


Figure 3. a) Light transmission spectra for the disordered microcavity BBABBAABBBABBBA/VO₂/BABAABBBABBBA (A = SiO₂; B = ZrO₂) with VO₂ in the

insulating phase (at 30 °C, black solid curve) and in the metallic phase (at 100 °C, blue dashed curve). b) Light transmission spectra for the microcavity $(\text{SiO}_2/\text{ZrO}_2)_5/\text{VO}_2/(\text{ZrO}_2/\text{SiO}_2)_5$, in which a random variation of the thicknesses is introduced, with VO_2 in the insulating phase (at 30 °C, black solid curve) and in the metallic phase (at 100 °C, blue dashed curve).

Also in Figure 3 the black solid curves correspond to the insulating phase of VO_2 , while the blue dashed curves to the metallic phase of VO_2 . In Figure 3a the transmission spectra for the disordered microcavity, in which VO_2 is embedded between one-dimensional random photonic structures [24,25]. The proposed structure follows the sequence BBABBAABBBABBBBA/ VO_2 /BABAABBBBABBABA. Also in this case, the layer thicknesses are the same of the ones of the periodic structure. The transmission spectrum with VO_2 in the insulating phase shows eight peaks in the studied range (900 – 2000 nm). With the transition from insulator to metal the suppression of most of the transmission peaks is noticeable.

In Figure 3b is shown the transmission spectra of the microcavity $(\text{SiO}_2/\text{ZrO}_2)_5/\text{VO}_2/(\text{ZrO}_2/\text{SiO}_2)_5$, in which a random variation of the thicknesses is introduced [26,27]. For the SiO_2 layers the thickness is $[2 \times (110 \pm n)]$, while for the ZrO_2 layers the thickness is $[1.5 \times (110 \pm n)]$, where n is an integer random number between 0 and 20. The transmission spectrum for the microcavity with vanadium dioxide in the insulating phase shows a manifold of transmission valleys and peaks. The transition from insulator to metal suppresses several transmission peaks, as for example the narrow peak at 1200 nm.

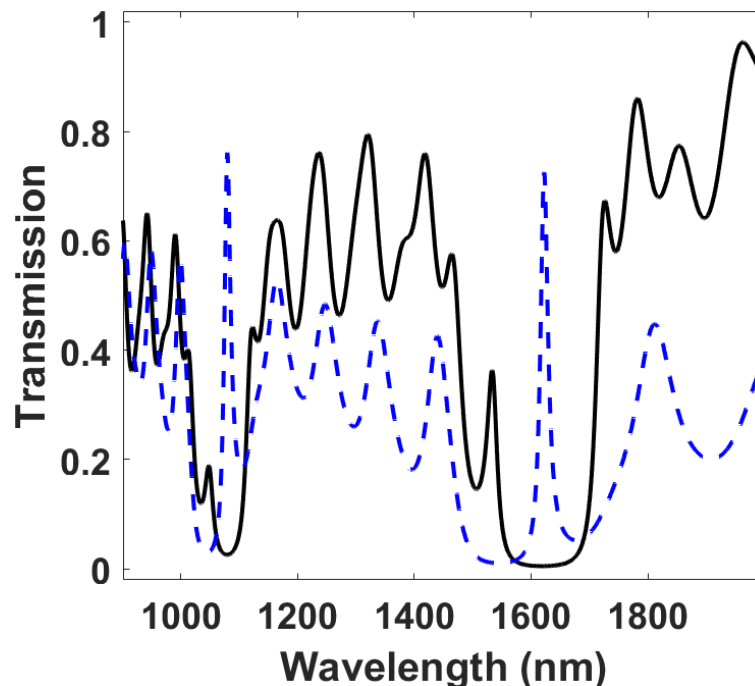


Figure 4. Light transmission spectra for the four material photonic crystal based microcavity $(\text{SiO}_2/\text{Al}_2\text{O}_3/\text{Y}_2\text{O}_3/\text{ZrO}_2)_6/\text{VO}_2/(\text{ZrO}_2/\text{Y}_2\text{O}_3/\text{Al}_2\text{O}_3/\text{SiO}_2)_6$ with VO_2 in the insulating phase (at 30 °C, black solid curve) and in the metallic phase (at 100 °C, blue dashed curve).

In Figure 4 the transmission spectrum of the four material-based microcavity $(\text{SiO}_2/\text{Al}_2\text{O}_3/\text{Y}_2\text{O}_3/\text{ZrO}_2)_6/\text{VO}_2/(\text{ZrO}_2/\text{Y}_2\text{O}_3/\text{Al}_2\text{O}_3/\text{SiO}_2)_6$ is shown. The thickness of SiO_2 layers is 275.9 nm, the thickness of Al_2O_3 layers is 228.6 nm, the thickness of Y_2O_3 layers is 210.5 nm, the thickness of ZrO_2 layers is 190.5 nm, and the thickness of VO_2 layers is 45.9 nm. As shown in previous reports,

four-material photonic crystals show a manifold of gaps [28]. In fact, with this structure, in the wavelength interval between 900 nm and 2000 nm two intense photonic band gaps are observable, compared to the single photonic band gap of the microcavity (Figure 1). In this case, the defect modes of the two photonic band gaps show a red shift and a remarkable intensity increase.

Conclusion

In this work it has been studied the light transmission of different one-dimensional photonic microcavities that embed vanadium dioxide by means of the transfer matrix method. The four types of microcavities include periodic photonic crystals, aperiodic structures, disordered structures, and four-material-based photonic crystals. The transmission of VO₂ from insulator to metal, achievable via a temperature increase, leads to a modulation of the transmission spectra, noticeable with shifts and suppressions of transmission peaks. The modulation of the transmission spectra of the microcavities can be exploited for smart windows and temperature controlled switches. Moreover, the photonic structure can be also used as temperature sensor since it has been studied by Currie et al. the temperature dependent refractive index dispersion of vanadium dioxide [3].

References

- [1] F.J. Morin, Oxides Which Show a Metal-to-Insulator Transition at the Neel Temperature, *Phys. Rev. Lett.* 3 (1959) 34–36. <https://doi.org/10.1103/PhysRevLett.3.34>.
- [2] R.M. Briggs, I.M. Pryce, H.A. Atwater, Compact silicon photonic waveguide modulator based on the vanadium dioxide metal-insulator phase transition, *Opt. Express*, OE. 18 (2010) 11192–11201. <https://doi.org/10.1364/OE.18.011192>.
- [3] M. Currie, M.A. Mastro, V.D. Wheeler, Characterizing the tunable refractive index of vanadium dioxide, *Opt. Mater. Express*, OME. 7 (2017) 1697–1707. <https://doi.org/10.1364/OME.7.001697>.
- [4] H.W. Verleur, A.S. Barker, C.N. Berglund, Optical Properties of V₂O₅ between 0.25 and 5 eV, *Phys. Rev.* 172 (1968) 788–798. <https://doi.org/10.1103/PhysRev.172.788>.
- [5] K. Liu, S. Lee, S. Yang, O. Delaire, J. Wu, Recent progresses on physics and applications of vanadium dioxide, *Materials Today*. 21 (2018) 875–896. <https://doi.org/10.1016/j.mattod.2018.03.029>.
- [6] H. Lu, S. Clark, Y. Guo, J. Robertson, The metal–insulator phase change in vanadium dioxide and its applications, *Journal of Applied Physics*. 129 (2021) 240902. <https://doi.org/10.1063/5.0027674>.
- [7] S. John, Strong localization of photons in certain disordered dielectric superlattices, *Phys. Rev. Lett.* 58 (1987) 2486–2489. <https://doi.org/10.1103/PhysRevLett.58.2486>.
- [8] E. Yablonovitch, Inhibited Spontaneous Emission in Solid-State Physics and Electronics, *Phys. Rev. Lett.* 58 (1987) 2059–2062. <https://doi.org/10.1103/PhysRevLett.58.2059>.
- [9] J.D. Joannopoulos, ed., *Photonic crystals: molding the flow of light*, 2nd ed, Princeton University Press, Princeton, 2008.
- [10] C. Toccafondi, L. Occhi, O. Cavalleri, A. Penco, R. Castagna, A. Bianco, C. Bertarelli, D. Comoretto, M. Canepa, Photochromic and photomechanical responses of an amorphous diarylethene-based polymer: a spectroscopic ellipsometry investigation of ultrathin films, *J. Mater. Chem. C*. 2 (2014) 4692–4698. <https://doi.org/10.1039/C4TC00371C>.
- [11] P. Guo, R.D. Schaller, L.E. Ocola, B.T. Diroll, J.B. Ketterson, R.P.H. Chang, Large optical nonlinearity of ITO nanorods for sub-picosecond all-optical modulation of the full-visible spectrum, *Nat Commun.* 7 (2016) 12892_1-12892_10. <https://doi.org/10.1038/ncomms12892>.

- [12] I. Kriegel, C. Urso, D. Viola, L. De Trizio, F. Scotognella, G. Cerullo, L. Manna, Ultrafast Photodoping and Plasmon Dynamics in Fluorine–Indium Codoped Cadmium Oxide Nanocrystals for All-Optical Signal Manipulation at Optical Communication Wavelengths, *J. Phys. Chem. Lett.* 7 (2016) 3873–3881. <https://doi.org/10.1021/acs.jpcllett.6b01904>.
- [13] I. Kriegel, F. Scotognella, Light-induced switching in pDTE–FICO 1D photonic structures, *Optics Communications*. 410 (2018) 703–706. <https://doi.org/10.1016/j.optcom.2017.11.019>.
- [14] Y.G. Boucher, A. Chiasera, M. Ferrari, G.C. Righini, Photoluminescence spectra of an optically pumped erbium-doped micro-cavity with SiO₂/TiO₂ distributed Bragg reflectors, *Journal of Luminescence*. 129 (2009) 1989–1993. <https://doi.org/10.1016/j.jlumin.2009.04.085>.
- [15] M. Born, E. Wolf, A.B. Bhatia, P.C. Clemmow, D. Gabor, A.R. Stokes, A.M. Taylor, P.A. Wayman, W.L. Wilcock, *Principles of Optics: Electromagnetic Theory of Propagation, Interference and Diffraction of Light*, 7th ed., Cambridge University Press, 1999. <https://doi.org/10.1017/CBO9781139644181>.
- [16] X. Xiao, W. Wenjun, L. Shuhong, Z. Wanquan, Z. Dong, D. Qianqian, G. Xuexi, Z. Bingyuan, Investigation of defect modes with Al₂O₃ and TiO₂ in one-dimensional photonic crystals, *Optik*. 127 (2016) 135–138. <https://doi.org/10.1016/j.ijleo.2015.10.005>.
- [17] G.M. Paternò, L. Moscardi, S. Donini, D. Ariodanti, I. Kriegel, M. Zani, E. Parisini, F. Scotognella, G. Lanzani, Hybrid One-Dimensional Plasmonic–Photonic Crystals for Optical Detection of Bacterial Contaminants, *J. Phys. Chem. Lett.* 10 (2019) 4980–4986. <https://doi.org/10.1021/acs.jpcllett.9b01612>.
- [18] I.H. Malitson, Interspecimen Comparison of the Refractive Index of Fused Silica*, †, *J. Opt. Soc. Am.*, JOSA. 55 (1965) 1205–1209. <https://doi.org/10.1364/JOSA.55.001205>.
- [19] C.Z. Tan, Determination of refractive index of silica glass for infrared wavelengths by IR spectroscopy, *Journal of Non-Crystalline Solids*. 223 (1998) 158–163. [https://doi.org/10.1016/S0022-3093\(97\)00438-9](https://doi.org/10.1016/S0022-3093(97)00438-9).
- [20] I.H. Malitson, Refraction and Dispersion of Synthetic Sapphire, *J. Opt. Soc. Am.*, JOSA. 52 (1962) 1377–1379. <https://doi.org/10.1364/JOSA.52.001377>.
- [21] Y. Nigara, Measurement of the Optical Constants of Yttrium Oxide, *Jpn. J. Appl. Phys.* 7 (1968) 404. <https://doi.org/10.1143/JJAP.7.404>.
- [22] D.L. Wood, K. Nassau, Refractive index of cubic zirconia stabilized with yttria, *Appl. Opt.*, AO. 21 (1982) 2978–2981. <https://doi.org/10.1364/AO.21.002978>.
- [23] W. Steurer, D. Sutter-Widmer, Photonic and phononic quasicrystals, *J. Phys. D: Appl. Phys.* 40 (2007) R229–R247. <https://doi.org/10.1088/0022-3727/40/13/R01>.
- [24] D.S. Wiersma, Disordered photonics, *Nature Photonics*. 7 (2013) 188–196. <https://doi.org/10.1038/nphoton.2013.29>.
- [25] D.S. Wiersma, R. Sapienza, S. Mujumdar, M. Colocci, M. Ghulinyan, L. Pavesi, Optics of nanostructured dielectrics, *J. Opt. A: Pure Appl. Opt.* 7 (2005) S190–S197. <https://doi.org/10.1088/1464-4258/7/2/025>.
- [26] J. Faist, J. -D. Ganière, Ph. Buffat, S. Sampson, F. -K. Reinhart, Characterization of GaAs/(GaAs)_n(AlAs)_m surface-emitting laser structures through reflectivity and high-resolution electron microscopy measurements, *Journal of Applied Physics*. 66 (1989) 1023–1032. <https://doi.org/10.1063/1.343488>.
- [27] A. Chiasera, F. Scotognella, L. Criante, S. Varas, G.D. Valle, R. Ramponi, M. Ferrari, Disorder in Photonic Structures Induced by Random Layer Thickness, *Sci Adv Mater.* 7 (2015) 1207–1212. <https://doi.org/10.1166/sam.2015.2249>.
- [28] I. Kriegel, F. Scotognella, Band gap splitting and average transmission lowering in ordered and disordered one-dimensional photonic structures composed by more than two materials

with the same optical thickness, *Optics Communications*. 338 (2015) 523–527.
<https://doi.org/10.1016/j.optcom.2014.10.045>.